

Simulation of Beamforming by Massive MIMO Antennas in Dense Urban Environments

Gregory J. Skidmore, Dr. Gary Bedrosian

Remcom, Inc.
State College, PA U.S.

Abstract – This paper presents a new predictive capability for simulating massive MIMO antennas and beamforming in dense urban environments. In anticipation of rapid growth in wireless devices and mobile data demand, Multiple input, multiple output (MIMO) is one of the key technologies being researched for 5G. This includes massive MIMO, which would allow base stations to use beamforming techniques to transmit data to multiple users in close proximity over a single frequency. New channel models are required to design, assess, and plan for these systems, as traditional approaches are unable to predict many of the key characteristics for MIMO channels, and more detailed methods suffer from significant computational burden due to the number of antennas in a massive MIMO array. To address this, an optimized simulation approach is presented for efficiently simulating the detailed multipath for large numbers of MIMO channels using ray-tracing, while overcoming the limitations and computational burden of traditional ray-tracing methods. The model is used to predict channel characteristics for an urban small cell scenario. Further calculations use maximum ratio transmission (MRT) and zero-forcing (ZF) beamforming to predict and visualize the beams to multiple mobile devices. Signal power and interference are evaluated, including the impacts to beamforming when pilot contamination is present. The combined results illustrate some of the complexities of massive MIMO systems, and demonstrate a new simulation approach for predicting and assessing their performance.

Index Terms – Massive MIMO, channel modeling, beamforming, Maximum ratio transmission (MRT), zero forcing (ZF), space-division multiple access (SDMA), pilot contamination.

I. INTRODUCTION

The telecommunications industry is anticipating rapid growth in the number of connected devices and the mobile data demand over the next decade. Typical estimates suggest that networks will need to support 1000 times higher data volume per area, 10 to 100 times more connected devices, and 10 to 100 times higher data rates [1]. To meet these demands, the industry is converging on a number of solutions for the next generation of wireless data network technology, 5G, including increased spectrum, and improved efficiency in how that spectrum is used. A key technology solution is multiple input, multiple output (MIMO), including *massive MIMO*, which uses large antenna arrays along with beamforming

techniques to provide data streams to multiple users within the same frequency band. However, applying these techniques successfully in urban environments is complex due to the large amount of multipath; traditional tools and methods for channel modeling are simply unable to predict many of the key channel characteristics for MIMO antennas.

Several organizations worldwide are researching and developing new models for 5G as described in [2]. METIS, one such organization, has defined key requirements for channel models in [3], including the following required improvements to support massive MIMO:

- (1) Ability to handle varying propagation conditions over a large array, requiring details of:
 - Azimuth and elevation angles of paths
 - Spherical wave fronts
 - Handling of 3D polarization of waves
- (2) Spatial consistency between different terminals and different positions while in motion

A three-dimensional ray-tracing solution can address each of these items by calculating the propagation paths through a simulated environment; however, a critical challenge is the computational load required to predict these details from each element of a large array, to many terminals, each potentially with their own MIMO antenna arrays. Traditional ray-tracing requires a simulation for each transmitting antenna in the array, which is computationally intensive for massive MIMO.

Another aspect of massive MIMO is the use of beamforming techniques to transmit different signals to different users simultaneously in the same frequency band, a process known as space-division multiple access (SDMA). An introduction to the mathematical techniques for beamforming can be found in [4]. It can be shown that the general beamforming optimization problem is an NP-hard computational task [5], or in simpler terms, it will likely take a computer algorithm longer to solve the problem of finding optimal weights than the time available before the users change locations and new sets of weights are required. For this reason, the development of efficient approximate or heuristic algorithms for beamforming is an active research area [6]-[9]. Research in these areas requires that a channel model calculate sufficient channel data to support beamforming algorithms.

This paper was presented by Remcom at the 2016 Electronic Design Innovation Conference in Boston, MA.

In this paper, we present an innovative and optimized approach for efficiently simulating the detailed multipath of large numbers of MIMO channels using ray-tracing, while overcoming the limitations and computational burden of traditional ray-tracing methods. Our study uses this new model to predict the complex channel characteristics between a massive MIMO base station and several mobile devices within an urban small cell with significant multipath. This is followed by analysis using techniques such as maximum ratio transmission (MRT) and zero-forcing (ZF) beamforming to predict the ability of beamforming to transmit signals to multiple users, including a scenario to predict the impact of pilot contamination from a mobile device in a neighboring cell. The capabilities of this unique approach allow the calculation of signal-to-interference-plus-noise ratio (SINR) to each device, as well as the actual physical beams formed using these techniques. The results provide new insight into some of the key problems and complexities faced by massive MIMO systems, and demonstrate a new simulation approach that can be used to predict and assess the performance of massive MIMO systems.

II. METHODS

A. Channel Modeling using Ray-Tracing

Ray-tracing is a common method for predicting power and path gain for wireless channels. It is particularly adept at predicting multipath in urban or indoor environments, where reflections from surfaces, diffractions around corners, and transmissions through materials create large numbers of propagation paths between transmitting and receiving antennas. The total power from the paths can be expressed as [10]:

$$P_R = \sum_{i=1}^{N_{paths}} \frac{\lambda^2}{8\pi\eta_0} |E_{\theta,i} g_{\theta}(\theta_i, \phi_i) + E_{\phi,i} g_{\phi}(\theta_i, \phi_i)|^2$$

where N_{paths} is the number of propagation paths, E_{θ} and E_{ϕ} are theta and phi polarized field components of each path, and g_{θ} and g_{ϕ} are the component gains.

Figure 1 shows an example of simulation results calculated using three-dimensional ray-tracing from Remcom's Wireless InSite® suite. A field map is overlaid on the urban scene, showing the received power at sensors placed approximately one meter apart at street level. Also shown are the strongest propagation paths to a sample point and the corresponding complex impulse response (received power vs. time of arrival of each path).

B. Optimized & Accelerated Ray-Tracing Method for Simulating Massive MIMO Arrays

For MIMO simulations, ray-tracing can provide details of the magnitude, phase, and time of arrival of individual propagation paths, which are the key elements of the MIMO channel. However, to get this level of detail for each sub-channel from each transmitting element of a MIMO base station antenna requires the equivalent of one additional

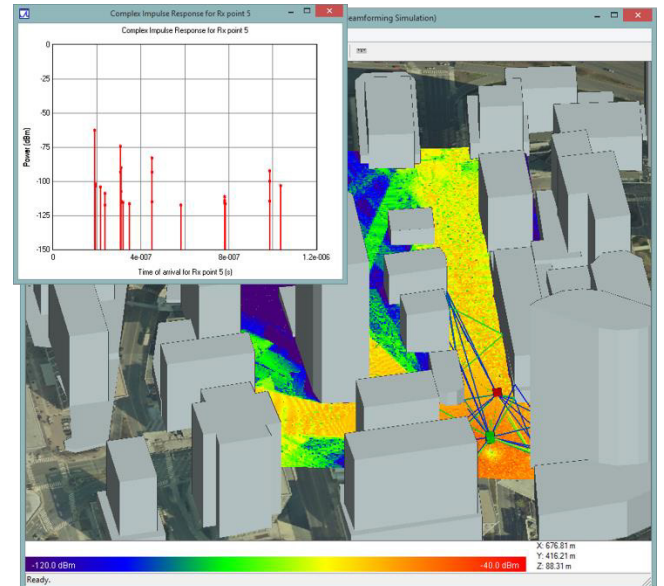


Figure 1. Field Map showing Multipath and Shadowing in an Urban Small Cell, including Paths and Complex Impulse Response to a Mobile Device (red).

simulation for each antenna in the MIMO array, with each simulation further complicated by the potential for additional MIMO antennas at the mobile devices. Ray-tracing simulations in a complex urban scene can already be computationally intensive. For a massive MIMO scenario, where there may be several base stations each with hundreds of antennas, simply increasing the simulations in this manner would not be practical.

This study presents the results of a new capability developed by Remcom, within its Wireless InSite® suite, that applies ray-tracing to efficiently simulate large MIMO arrays. The model has been built on an existing GPU-accelerated and optimized ray-tracing code. This has been extended using two Remcom proprietary techniques: *Adjacent Path Generation (APG)*, and exact path correction which together allow the exact propagation paths for every point in large, dense sets of transmitters or receivers to be found using a much reduced ray trace to a sparser sets of points.

The critical advantage of this technique over other approaches is that it retains detailed time of arrival and phase information for each path to each element, keeping the spherical or diffracted phase fronts in all calculations. This provides a high-fidelity solution for predicting how propagation channels vary for mobile devices moving through a scene under realistic multipath conditions. Meanwhile, the optimizations allow it to achieve this without significant increases to the run-time over simulations using single transmit and receive antennas.

C. Beamforming Techniques

Optimal beamforming is a compromise between delivering the maximum power to an individual user, and reducing or eliminating the interference of the signal at the

other users. If the maximum power is delivered to user k , the interference to the other users is uncontrolled and likely to be relatively high for users close to user k . On the other hand, if interference to the other users is reduced, the power reaching user k could also be reduced for a given total transmit power. The optimum solution is between these two extremes [4], making them useful as limiting cases. The remainder of this section provides a brief overview of the mathematical techniques for beamforming used in this study.

The summary uses the mathematical development in [4]. In the discussion, n is the index of a base station antenna element and k is the index of a user. $G_k[n]$ is the ratio of the power received by user k divided by the power radiated by element n with all other elements radiating zero power. $\theta_k[n]$ is the phase in radians of the voltage across a matched load at k under the same conditions. Note that $G_k[n]$ and $\theta_k[n]$ include all of the propagation paths in a complex urban environment from antenna element n to user k summed coherently. The propagation factor, $g_k[n]$, is defined as

$$g_k[n] \equiv \sqrt{G_k[n]} e^{j\theta_k[n]}$$

When written in **bold** without the $[n]$, \mathbf{g}_k is an N -dimensional complex row vector ($1 \times N$). Closely associated with \mathbf{g}_k is the channel vector \mathbf{h}_k , an N -dimensional complex column vector ($N \times 1$) given by

$$\mathbf{h}_k = \mathbf{g}_k^*$$

where $*$ denotes the conjugate transpose. The antenna element weight vector for user k is \mathbf{w}_k , also an N -dimensional complex column vector.

Maximum power to user k is achieved when the weights of the antenna elements are proportional to the channel values of the respective elements. This arrangement is known as *maximum ratio transmission*, or MRT, and is a relatively simple beamforming solution. Defining p_k as the total power allocated for transmission to user k , the antenna element weight vector for user k is given by

$$\mathbf{w}_k = \frac{\mathbf{h}_k}{|\mathbf{h}_k|} \sqrt{p_k}$$

Minimizing interference is termed *zero-forcing (ZF) beamforming*. As the name implies, the objective is to set the weights of the antenna elements for user k so that all of the other users are in local nulls. Calculation of ZF beamforming is more complicated than MRT. Let $\mathbf{H} = [\mathbf{h}_1, \dots, \mathbf{h}_K]$ be the collection of all channel column vectors into one ($N \times K$) matrix. Similarly, let $\mathbf{W} = [\mathbf{w}_1, \dots, \mathbf{w}_K]$ be the collection of all column vector antenna element weights into one ($N \times K$) weight matrix. $\mathbf{\Lambda}$ is a ($K \times K$) diagonal matrix of optimization weights λ_i for each user; λ_i represents the importance of interference from signals meant for user i relative to other sources of noise and interference. \mathbf{P} is a ($K \times K$) diagonal matrix of power allocations for each user. The ZF beamforming antenna element weight matrix is

$$\mathbf{W} = \mathbf{H}(\mathbf{H}^* \mathbf{H})^{-1} \mathbf{\Lambda}^{-1} \sqrt{\mathbf{P}}$$

Once the matrix of antenna weights, \mathbf{W} , has been determined and the signals to be sent to each user are known, \mathbf{W} is scaled up or down to meet constraints on total power, and possibly to apply power to each mobile device according to a power allocation scheme.

D. Received Power and SINR for Multi-User MIMO

When the MRT and ZF beamforming techniques are used in a Multi-user MIMO system, the base station transmits a signal to each user, k , according to its weight vector. The resultant power received by each user for the signal intended for that user is calculated as the product of the channel gain and this weight vector:

$$Pr_k = |\mathbf{g}_k \mathbf{w}_k|^2 = |\mathbf{h}_k^* \mathbf{w}_k|^2$$

Because the MIMO system transmits to multiple users at the same frequency, a critical performance metric for the system is the *signal-to-interference-plus-noise ratio (SINR)* for each user. This is calculated as:

$$\text{SINR}_k = \frac{|\mathbf{g}_k \mathbf{w}_k|^2}{\sum_{i \neq k} |\mathbf{g}_k \mathbf{w}_i|^2 + \sigma^2} = \frac{|\mathbf{h}_k^* \mathbf{w}_k|^2}{\sum_{i \neq k} |\mathbf{h}_k^* \mathbf{w}_i|^2 + \sigma^2}$$

The first term in the denominator represents interference from transmissions to other users, and the second represents random noise.

E. Pilot Contamination

The base station estimates the channels from pilot sequences transmitted by each mobile device. Using the principle of reciprocity and calibration techniques, the base station can use this to determine the channel vectors, \mathbf{h}_k , for each user within the cell. Ideally, each terminal will have an orthogonal pilot sequence; however, the number of possible pilot sequences is limited by the coherence interval [11], [12]. With multiple cells and large numbers of mobile terminals, this number can be quickly reached, requiring adjacent cells to reuse pilot sequences.

When a base station receives identical or correlated pilot sequences from more than one terminal, it is referred to as *pilot contamination*. This condition can degrade the channel estimates, reducing the performance of beamforming within the cell, while also potentially increasing the interference to the terminal in the neighboring cell as the base station directs more of the signal toward that terminal [11], [13].

Mathematically, the effect of pilot contamination on the estimated channel vector can be described as follows:

$$h_k = \sum_{p=1}^P h_{k,p}$$

where p refers to the terminals within range of the base station that are using the same pilot sequence, k . The beamforming

weight vectors are calculated as described above. However, treating the first user as the one within the cell, the SINR to user $k, 1$ is modified to the following:

$$SINR_{k,1} = \frac{|\mathbf{h}_{k,1} * \mathbf{w}_k|^2}{\sum_{i \neq k}^K |\mathbf{h}_{k,i} * \mathbf{w}_i|^2 + \sigma^2}$$

Of the signal directed toward user $k, 1$, the amount that instead manifests as interference to user k, p in a neighboring cell is

$$I_{k,p} = |\mathbf{h}_{k,p} * \mathbf{w}_k|^2$$

The total interference to user k, p from all signals directed to users in the local cell is

$$I_{k,p} = \sum_{i=1}^K |\mathbf{h}_{k,p} * \mathbf{w}_i|^2$$

III. RESULTS & DISCUSSION: SIMULATION OF MASSIVE MIMO IN AN URBAN SCENE

A. Scenario: Urban Small Cell Base Station with MIMO Antenna

To demonstrate MIMO simulation concepts described in Section II, a small cell scenario was set up in a dense urban environment, in Rosslyn, Virginia. Figure 2 shows the base station, positioned atop a post on a median in a major intersection. This was defined to have an 8x8 array with both vertically and horizontally polarized antennas, for a total of 128 elements. Receivers were positioned at 15 stationary locations, depicted in red, in addition to a mobile device moving along a route through the scene, shown as a red line. A 17th mobile device, shaded blue, was used for a pilot contamination scenario, described later. For simplicity, these devices were specified to have vertical dipole antennas, though patch antennas, MIMO arrays, or other types would have been supported by the model.

Table 1: Key Specifications for Scenario

Parameter	Definition	Notes
Frequency	28 GHz	
Base Station Antenna	128-Element MIMO Array	8x8, with cross-pol elements
B. S. Height	10 m	(Atop lamp post)
Rx Antennas	Vertical dipoles	
Rx Heights	1.5m AGL	

As a baseline simulation, Wireless InSite was first used to simulate a single-input-single-output (SISO) configuration, with a single dipole antenna at the base station as well. Figure 1 shows sample results. The field map, dominant paths to a sample point, and the plot of complex impulse response all demonstrate the large amount of multipath and shadowing present in the urban scene.

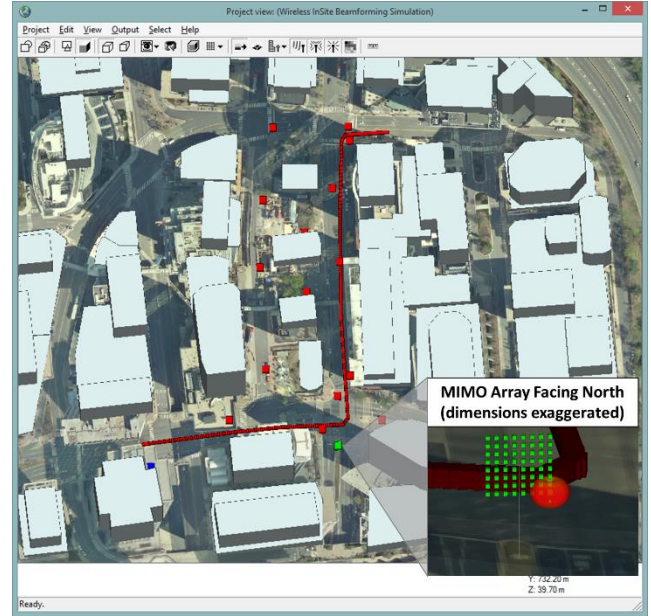


Figure 2: Base Station with MIMO antenna and users within small cell in Rosslyn, VA

B. Massive MIMO Simulations

Next, the Wireless InSite® MIMO capability was used to simulate propagation from the massive MIMO array. This calculated the complex channel vectors, \mathbf{h}_k , to each stationary and mobile device, as well as to all of the points in the field map. Although complex channel vectors are difficult to visualize, the squares of their magnitudes constitute the path gain for the sub-channel between each base station antenna element, and each receiver antenna element. Figure 3 shows a plot of path gain for the 128 sub-channels between the base station and the mobile device moving along the route. The cluster with higher path gains is from transmit antennas that were vertically polarized (matching the polarization of the receiver). The cluster with lower path gains is from transmit antennas that were horizontally polarized.

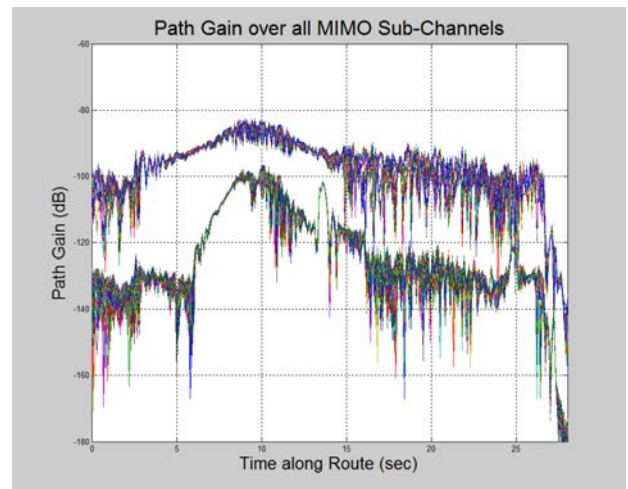


Figure 3. Path Gain to Mobile Device along Route for all 128 MIMO Sub-channels

C. Beamforming with MRT and ZF

The complex path gains were obtained from the simulation results and used to calculate beams using the MRT and ZF beamforming techniques described in Section II.C. For this analysis, the h-vectors (path gains) were obtained for 16 mobile devices: 15 at stationary points and one moving along a route, as shown Figure 2. Post-processing tools were developed to generate beamforming and assess statistics, using the Matlab scripts provided by the authors of [4] to calculate the beamforming weighting vectors, w , for the MRT and ZF beamforming techniques. These were calculated for each point in time as the device moved along its route. They were then applied to the path gain matrix for the field map in order to display the beams generated for the mobile device at each point in time.

Figure 4 shows examples of the beams formed to the mobile device at two points along its route. In each display, the base station is a large green dot, and the device toward which the beam is directed is shown as a large red dot. The other devices are smaller red circles. At each point in time, there are clear beams to the intended device, though side lobes and multipath (reflections and diffractions from buildings) send strong signals in other directions as well. With the MRT technique, the beam to the intended receiver is strong, but it is clear that the technique makes no attempt to prevent interference to the other receivers. The ZF technique, on the other hand, is extremely successful in suppressing the signal to the other receivers, creating nulls around their positions.

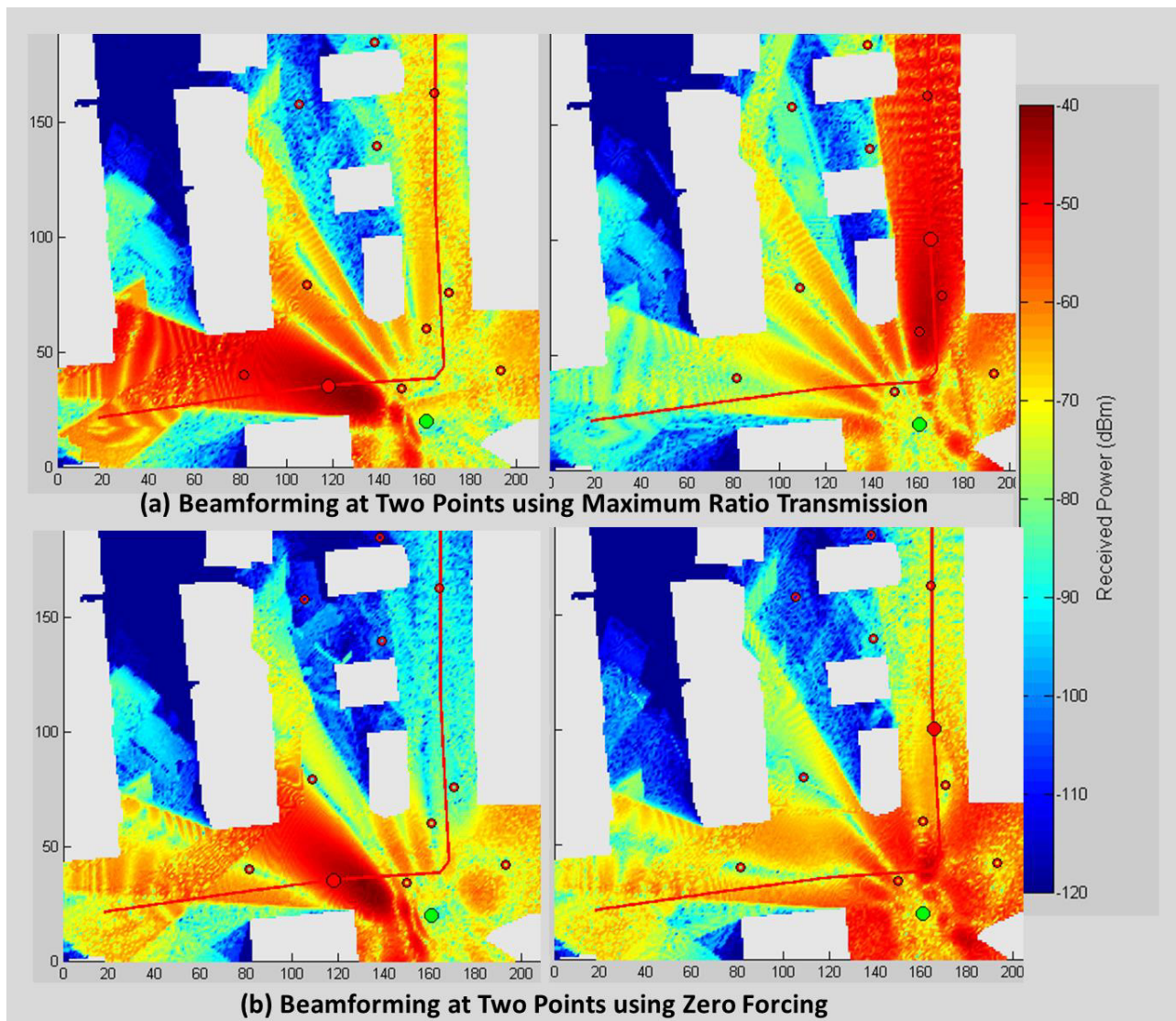


Figure 4: Beams created to the Mobile Device using MRT and ZF at Two Points in Time along its Route

Signal-to-Interference-Plus-Noise (SINR) was calculated for the full set of route points, according to the formulas in section III.D. The value for noise was obtained from [14] using the vertically-polarized measured noise value for urban areas, scaled to assume a 100MHz bandwidth; this resulted in a noise floor of -87.1 dBm. Mean values for the received signal power, the received interference power (from signals intended for other devices), and the SINR are provided in Table 2, below. As these show, the signal power to the intended receiver is stronger with MRT than with ZF by approximately 13dB; however, the interference to other receivers is stronger still, such that overall SINR to users in the cell is best by far when the ZF technique is used.

Table 2: Received Power and SINR

	Mean Values over Route	MRT	ZF
Moving Device	Received Pwr (dBm)	-49.0	-63.0
	Interference (dBm)	-47.9	Neg.*
	SINR (dB)	-3.7	21.6
Stationary Devices	Received Pwr (dBm)	-54.1	-69.4
	Interference (dBm)	-53.4	Neg.*
	SINR (dB)	-3.3	15.2

*Interference for ZF was negligible (well below noise floor).

D. Beamforming with Pilot Contamination

Next, an additional receiver was placed in the southwest corner of the scene, shaded blue in Figure 5. Using the method described in Section II.E, the path gain h vectors were combined to simulate the condition in which this new mobile device, assumed to be in a neighboring cell, is transmitting the same pilot sequence as the mobile device moving along the route. Overall, this had the following effects on the results:

- 1.) It reduced the strength of the signal to the intended device at many points along the route
- 2.) For ZF beamforming, it increased the interference to this intended device from all of the other devices in the cell (no longer effectively zero-forcing to it)
- 3.) It redirected some of the signal from the intended device to interfere with the neighboring device (blue)

Figure 5 shows a sample point in time, where the signal along multiple paths to the intended device has noticeably dropped, while it has increased a small amount to the neighboring device with the interfering pilot signal.

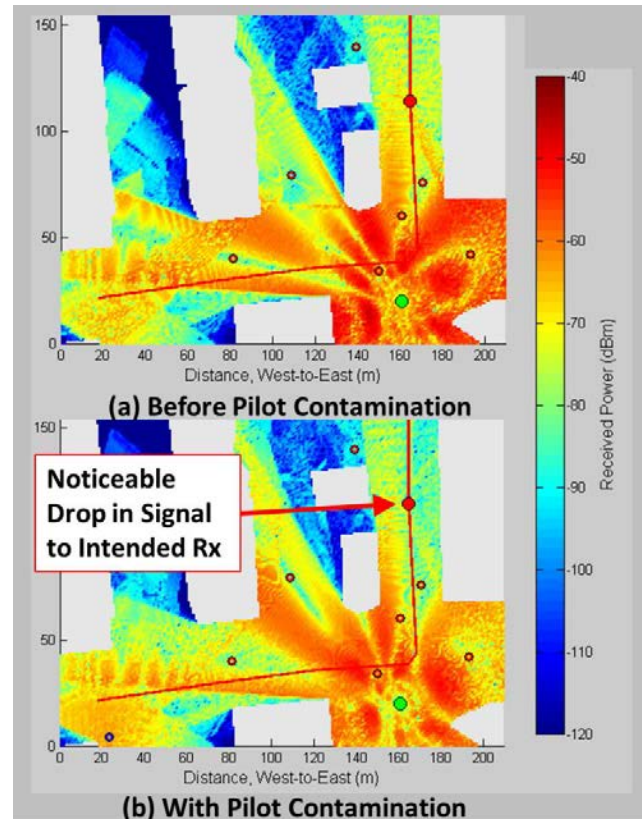


Figure 5: Pilot Contamination Partially Redirects Signal

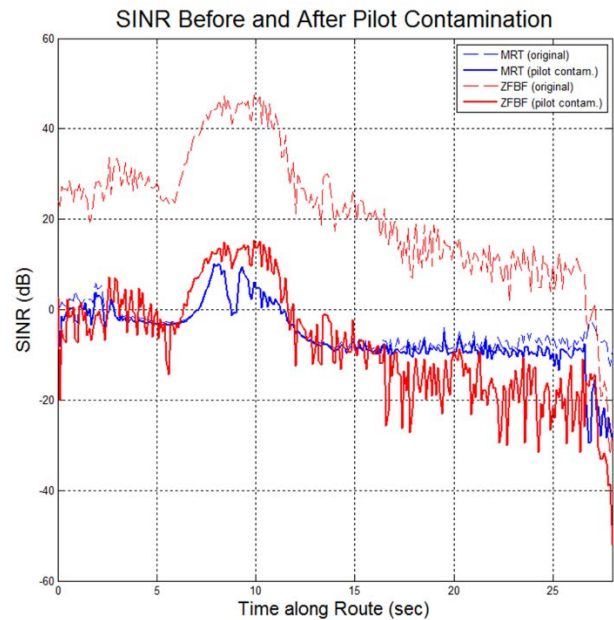


Figure 6: Pilot Contamination Route Significantly Reduces SINR for the Zero-Forcing Beamforming Technique

Table 3 shows the change in signal power, interference, and SINR to the mobile device on the route. With the MRT technique, there is a minor reduction in the mean power, resulting in a small reduction in the SINR. With ZF, on the other hand, the change is dramatic; the mean received power drops approximately 5.6dB, while the interference increases from a negligible level to stronger than the actual signal. The combination drops the mean SINR approximately 29dB. This can be seen clearly in Figure 6, which shows the SINR as a function of time along the route for both techniques. The lighter shaded lines are prior to pilot contamination, and the more solid lines are after. Clearly the ZF technique (in red), is significantly affected across the entire route, whereas the effect to the MRT technique appears to be minor.

Table 3: Power & SINR with Pilot Contamination

Beam	Mean Values over Route	Original	Pilot Cont.	Chg.
MRT	Rcvd. Pwr. (dBm)	-49.0	-51.0	-1.9
	Interference (dBm)	-47.9	-47.9	0
	SINR (dB)	-3.7	-5.6	-1.9
ZF	Rcvd. Pwr. (dBm)	-63.0	-68.6	-5.6
	Interference (dBm)	Neg.*	-64.2	High*
	SINR (dB)	21.6	-7.6	-29.1

*Interference for ZF increases from well below noise floor to above signal, significantly reducing SINR.

The pilot contamination also increases interference to the device in the neighboring cell. Table 4 shows a comparison of the mean power of the interfering signal received by the neighboring device that was intended for the device within the cell. For both beamforming techniques, the interference increases significantly after pilot contamination is introduced (9-12dB).

Table 4: Interference to Neighboring Device

Method	Mean Values over Route	Orig.	Pilot Cont.	Change
MRT	Interference (dBm)	-75.1	-62.6	+12.4
ZF	Interference (dBm)	-73.3	-64.5	+8.8

E. Simulation Efficiency: Run-Time Comparisons

A key element of the Wireless InSite MIMO capability is its optimized methods to limit the growth of run-time for large MIMO antennas. Table 5 shows the execution times for the simulations in this study. Benchmarks were generated from simulations performed on a high-end workstation with an Intel i7-3770 CPU, an NVIDIA Quadro K620, and 32 GB of system RAM. The results are for a small sample of simulations, but

are presented as representative examples to demonstrate the capability.

The first column shows the results for the route and the 16 stationary points (317 points, total). This is the actual simulation that would need to be performed to evaluate the performance of the small cell for the mobile devices in the scenario. The second column shows the results for the field map, which had a large number of points (approximately 65,621). Its purpose was solely to visualize the beams directed toward each mobile device. The first three rows show measured run times for the following:

- Single antenna case before optimizations (baseline)
- Improvement due to APG acceleration
- Run time for the optimized MIMO simulations

The fourth row gives estimated execution times that would have been incurred if each of the 128 transmitting elements of the MIMO antenna had been simulated as a new base station antenna (the method required prior to the optimized MIMO capability).

The ratio of the estimate to the actual MIMO run time experienced in this study is the speed improvement factor offered by the optimized MIMO approach. For these two simulations sets, that factor was approximately 51X and 94X speed reduction, respectively. In other words, although there were 128 times as many transmitting antennas to simulate, the optimizations reduced the impact so that simulations were just slightly longer than those for a single antenna using the original version of the model. This reduced calculations that were performed to visualize the beamforming from an estimated three days (before optimizations) to just 49 minutes. The much shorter calculations to evaluate SINR and pilot contamination effects for the mobile devices completed in less than two minutes instead of running for over an hour. These quick run times allowed for many iterations in the analysis, and make this new capability very practical to apply to realistic scenarios, which could involve larger numbers of cells, mobile devices, and urban structures.

Table 5: Run Time Comparisons

Simulation Case	Mobile Devices (317 pts)	Field Map (66K pts)
Single Antennas (SISO)		
• Before optimizations	0.6 min	35.7 min
• APG accelerated	0.5 min	9.1 min
Optimized MIMO	1.6 min	48.6 min
MIMO: estimate <i>without</i> Optimizations	1hr, 19 min	4,572 min (~3 days)
Speed Improvement	51X	94X

IV. CONCLUSIONS

In this article, we have presented a new, efficient method for predicting multipath and channel characteristics for massive MIMO systems. Through additional calculations, we demonstrated how complex channel data can be extracted from the simulations and used to analyze MIMO performance, applying beamforming techniques and predicting the resultant received power and SINR. Optimizations provide efficient run times, which allow this new capability to be applied to realistic scenarios, including the ability to expand them to include multiple cells and greater numbers of mobile devices. These results demonstrate a new capability that can be practically applied to perform research and assess performance of massive MIMO systems in future 5G mobile networks.

V. REFERENCES

[1] A. Osserian et al., “Scenarios for the 5G Mobile and Wireless Communications: the Vision of the METIS Project,” *IEEE Communications Magazine*, Vol. 52, Issue 5, May 2014, pp. 26-35.

[2] K. Haneda et al., “Indoor 5G 3GPP-like Channel Models for Office and Shopping Mall Environments,” 2016 IEEE International Conference on Communications Workshops (ICC), 23-27 May 2016, pp. 694 - 699.

[3] V. Nurmela et al., “METIS Channel Model,” METIS, Document number ICT-317669-METIS/D1.4 v3, July 2015. https://www.metis2020.com/wp-content/uploads/METIS_D1.4_v3.pdf

[4] E. Björnson, M. Bengtsson, and B. Ottersten, “Optimal Multiuser Transmit Beamforming: A Difficult Problem with a Simple Solution Structure”, *IEEE Signal Processing Magazine*, Vol. 31, No. 4, 2014, pp. 142-148.

[5] Y. Liu, Y. Dai, and Z. Luo, “Coordinated Beamforming for MISO Interference Channel: Complexity Analysis and Efficient Algorithms”, *IEEE Transactions on Signal Processing*, Vol. 59, No. 3, 2011, pp. 1142-1157.

[6] D. Liu, W. Ma, S. Shao, Y. Shen, and Y. Tang, “Performance Analysis of TDD Reciprocity Calibration for Massive MU-MIMO Systems With ZF Beamforming”, *IEEE Communications Letters*, Vol. 20, No. 1, 2016, pp. 113-116.

[7] M. N. Kulkarni, A. Ghosh, and J. G. Andrews, “A Comparison of MIMO Techniques in Downlink Millimeter Wave Cellular Networks With Hybrid Beamforming”, *IEEE Transactions on Communications*, Vol. 64, No. 5, 2016, pp. 1952-1967.

[8] A. Puglielli et al., “Design of Energy- and Cost-Efficient Massive MIMO Arrays”, *Proceedings of the IEEE*, Vol. 104, No. 3, 2016, pp. 586-606.

[9] S. Kuttty and D. Sen, “Beamforming for Millimeter Wave Communications: An Inclusive Survey”, *IEEE Communications Surveys & Tutorials*, Vol. 104, No. 3, 2016, pp. 949-973.

[10] Remcom, Inc., “Wireless InSite Reference Manual, Version 2.8.1,” Remcom, Inc. Manual, July 2016, pp. 284.

[11] E. G. Larsson, F. Tufvesson, O. Edfors, and T. L. Marzetta, “Massive MIMO for next generation wireless systems,” *IEEE Commun. Mag.*, vol. 52, no. 2, pp. 186–195, Feb. 2014.

[12] T. L. Marzetta, “Noncooperative cellular wireless with unlimited numbers of base station antennas,” *IEEE Trans. Wireless Commun.*, vol. 9, no. 11, pp. 3590–3600, Nov. 2010.

[13] L. Lu, G. Y. Li, A. L. Swindlehurst, A. Ashikhmin, and R. Zhang, “An Overview of Massive MIMO: Benefits and Challenges,” *IEEE Journal of Selected Topics in Signal Processing*, Vol. 8, No. 5, October 2014, pp. 742-758.

[14] R. Beck, “Results of Ambient RF Environment and Noise Floor Measurements Taken in the U.S. in 2004 and 2005,” World Meteorological Organization Report, CBS/SG-RFC 2005/Doc. 5(1), March 2006.